

Heptyl α -D-mannosides grafted on a β -cyclodextrin core to interfere with *Escherichia coli* adhesion – an *in vivo* multivalent effect

Julie Bouckaert,^{*†§} Zhaoli Li,^{‡§} Catarina Xavier,¹ Mehdi Almant,^{||} Vicky Caveliers,¹ Tony Lahoutte,¹ Stephen D. Weeks,[‡] José Kovensky,^{||} and Sébastien G. Gouin^{*||#}

[†] *Unité de Glycobiologie Structurale et Fonctionnelle (UGSF), UMR8576 du CNRS, Université Lille 1, F-59655 Villeneuve d'Ascq Cedex, France,*

[‡] *Viral Genetics Research Group, Faculty of Science and Bio-engineering Sciences, Vrije Universiteit Brussel, Pleinlaan 2, 1050 Brussels, Belgium,*

¹ *In Vivo Cellular and Molecular Imaging (ICMI) Laboratory, Vrije Universiteit Brussel, Laarbeeklaan 103, 1090 Brussels, Belgium,*

[‡] *Laboratory for Biocrystallography, KU Leuven, Department of Pharmaceutical Sciences, O&N II Herestraat 49 - bus 822, 3000 Leuven, Belgium,*

^{||} *Laboratoire des Glucides FRE 3517, Institut de Chimie de Picardie, Faculté des Sciences, Université de Picardie Jules Verne, 33 rue Saint-Leu, 80039 Amiens Cedex 1, France,*

[#] *LUNAM Université, CEISAM, Chimie Et Interdisciplinarité, Synthèse, Analyse, Modélisation, UMR CNRS 6230, UFR des Sciences et des Techniques, 2, rue de la Houssinière, BP 92208, 44322 NANTES Cedex 3, France.*

Contents

General procedure for chemical synthesis	S2
Experimental procedures and characterizations of synthetic products	S3-S9
NMR spectra of synthetic products	S10-S17
Procedure and data for isothermal titration calorimetry (ITC)	S18-S21
Procedure and data for small angles X-ray solution scattering (SAXS) and (DLS)	S22-S25
Epifluorescence microscopy	S26
Dynamic imaging and pharmacodistribution	S27-S29
<i>In vivo</i> inhibition in a murine cystitis model	S30

General procedure for chemical synthesis: All purchased materials were used without further purification. Methylene chloride and DMF were distilled from calcium hydride, pyridine over KOH and tetrahydrofuran over sodium and benzophenone. Analytical thin layer chromatography (TLC) was carried out on Merck D.C.-Alufolien Kieselgel 60 F₂₅₄. Flash chromatography (FC) was performed on GEDURAN SI 60, 0.040-0.060 mm pore size using distilled solvents. ¹H, and ¹³C nuclear magnetic resonance (NMR) spectra were respectively recorded at 300 and 75.5 MHz with a Bruker AC-300 or at 600 and 150 MHz with a Bruker AC-600 spectrometer, and chemical shifts are reported in parts per million relative to tetramethylsilane or a residual solvent peak (CHCl₃: ¹H: δ=7.26, ¹³C: δ=77.2; DMSO-d₆: ¹H: δ=2.54, ¹³C: δ=40.4). Peak multiplicity is reported as: singlet (s), doublet (d), triplet (t), quartet (q), multiplet (m), and broad (br). High resolution mass spectra HRMS were obtained by Electrospray Ionisation (ESI) on a Micromass-Waters Q-TOF Ultima Global. Optical rotations were measured on a 343 PERKIN ELMER at 20°C in a 1cm cell in the stated solvent; [α]_D values are given in 10⁻¹ deg.cm² g⁻¹ (concentration c given as g/100 mL). Microwave irradiation was performed in a CEM Discover apparatus (300 W). Preparative reversed-phase HPLC was accomplished on a Waters PREP LC 4000 chromatography system with a (DEDL) PL-ELS 1000 photodiode array detector. All HPLC samples were purified on a preparative Prevail C-18 column (2.2 x 25 cm). The mobile phase was H₂O (solvent A) and MeOH (solvent B). The gradient consisted of 100% A for 10 min to 100% B in 30 min (22.0 mL.min⁻¹ flow rate).

Experimental procedures and characterizations of synthetic products

8-Oxaundec-10-ynyl 2,3,4,6-tetra-*O*-acetyl- α -D-mannopyranoside **8**

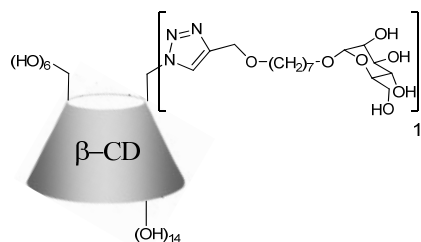
Mannosyl pentaacetate (229 mg, 0.587 mmol), compound **7** (150 mg, 0.882 mmol) and silver trifluoroacetate (194 mg, 0.878 mmol) were dissolved in dry dichloromethane (3 mL). A solution of SnCl₄ 1M in dichloromethane (585 μ L) was added and the mixture was stirred at rt for 3 h under argon atmosphere. The solution was diluted in dichloromethane (10 mL) and washed with NaHCO₃ satd. (2 x 10 mL). The organic layer was dried, filtered and evaporated under reduced pressure. The residue was chromatographed on silica gel with ethyl acetate-cyclohexane (2-8) to (3-7) to afford **8** as a colorless oil (128 mg, 44%). Analytical data were identical as previously described [Gouin, S.G.; Wellens, A.; Bouckaert, J.; Kovensky, J. *ChemMedChem*. **2009**, *5*, 749-55].

8-Oxaundec-10-ynyl- α -D-mannopyranoside **9**

8 (400 mg, 800 μ mol) was dissolved in MeOH (10 mL). A solution of freshly prepared sodium methanolate 1M in methanol (500 μ L) was added and the mixture was stirred at rt for 4h. Amberlyst IR120 (H⁺) was added and the mixture stirred until pH reached 5. The resin was filtered off and the solution was evaporated to dryness leading to unprotected product **10** (263 mg, 99%).

$[\alpha]_D = +96$ (c= 0.2, MeOH); ¹H NMR (300 MHz, CD₃OD) δ = 4.76 (1 H, d, J = 1.6 Hz, H-1), 4.14 (2 H, d, J = 2.4 Hz, OCH₂C), 3.82-3.80 (2 H, m, H-2, H-3), 3.75-3.69 (3 H, m, H-5, 2 x H-6), 3.64 (1 H, t, J = 9.3 Hz, H-4), 2.84 (1 H, t, CCH), 1.61-1.55 (4 H, br, 2 x CH₂), 1.39 (6 H, br, 6 x CH₂); ¹³C NMR (125 MHz, D₂O): δ = 102.4 (C1), 76.5 (CCH), 75.5, 73.5, 73.1, 71.8 (C-2, -3, -4, -5), 69.4 (CH₂O), 59.6 (CH₂CCH), 31.4, 31.3, 31.1, 28.1, 28.0 (CH₂); HRMS (ES⁺): Found 355.1732 C₁₆H₂₈O₇Na requires 355.1733.

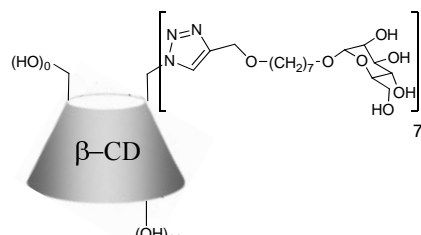
Compound 1



Alkynyl-saccharide **10** (29 mg, 87 μmol) and **11** (50 mg, 43 μmol) were dissolved in a DMF / H₂O mixture (2 / 0.5 mL). Copper sulfate (6.9 mg, 43 μmol) and sodium ascorbate (17 mg, 86 μmol) were added and the mixture was stirred at 70°C for 30 minutes under μW irradiation. Ethylenediamine tetraacetic acid trisodium salt (50 mg, 127 μmol) was added and the mixture was stirred for 10 minutes at rt. The mixture was evaporated under reduced pressure and the residue purified by preparative HPLC leading to **1** (33 mg, 51%) as a white powder after lyophilisation.

$[\alpha]_D = +130$ ($c = 0.1$, MeOH); Tr = 17 min; ^1H NMR (500 MHz, D₂O) $\delta = 8.23$ (1 H, s, H_{triazol}), 5.51, 5.36, 5.30 (7 H, 3s, H-1^{I-VII}), 5.15 (1 H, s, H-1^{HM}), 4.20-3.20 (54 H, br, H-2,-3,-4,-5,-6, ^{I-VII}, H-2,-3,-4,-5,-6^{HM}, O-CH₂-triazol, 2 x CH₂), 1.72, 1.65, 1.47 (10 H, br, (x CH₂), ^{13}C NMR (125 MHz, D₂O): $\delta = 146.1$ (C=CH_{triazol}), 123.8 (CH=C_{triazol}), 102.1, 101.8, 99.9 (C1^{I-VII}, C1^{HM}), 83.1, 81.7, 80.9, 80.3 (C4^{I-VII}), 72.1, 71.0, 70.4, 68.6, 67.0, 66.5, 63.0, 60.7, 59.8, 58.8 (C2,-3,-5^{I-VII}, C6^{II-VII}, C2,-3,-4,-5,-6^{HM}, CH₂O), 51.5 (C6^I), 29.1, 28.5, 28.0, 25.7, 25.1 (CH₂); HRMS (ES⁺): Found 1514.5564 C₅₈H₉₇N₃O₄₁Na requires 1514.5495.

Compound 2

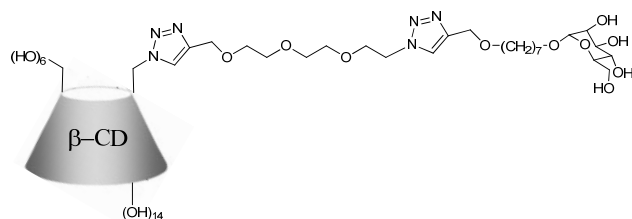


Alkynyl-saccharide **10** (48 mg, 144 μmol) and **12** (22 mg, 17.1 μmol) were dissolved in a DMF / H₂O mixture (2 / 0.5 mL). Copper sulfate (8.2 mg, 51 μmol) and sodium ascorbate (20 mg, 100 μmol) were added and the mixture was stirred at 70°C for 45 minutes under μW irradiation. An ethylenediamine tetraacetic acid trisodium salt solution (50 mg, 127 μmol) in water (5 mL) was added and the mixture was

stirred for 30 minutes at rt. The mixture was evaporated under reduced pressure and the residue purified by preparative HPLC leading to **2** (23 mg, 37%) as a white powder after lyophilisation.

$[\alpha]_D = +36$ ($c = 0.2$, H_2O); Tr = 34 min; 1H NMR (500 MHz, DMSO) $\delta = 7.91$ (7 H, s, H_{triazol}), 6.00-5.90 (9 H, br, OH), 5.06 (7 H, s, $H-1^{I-VII}$), 4.79, 4.69, 4.57, 4.50 (27 H, 4 s, 7 x $H-1^{HM}$, 20 x OH), 3.75-3.00 (90 H, m, $H-2,-3,-4,-5,-6^{I-VII}$, 7 x $-2,-3,-4,-5,-6^{HM}$, 7 x O-CH₂-triazol, 14 x OCH₂), 1.44, 1.36, 1.19 (70 H, br, CH₂), ^{13}C NMR (125 MHz, D₂O): $\delta = 144.0$ ($C=CH_{\text{triazol}}$), 125.2 ($CH=C_{\text{triazol}}$), 101.6 ($C1^{I-VII}$), 99.7 ($C1^{HM}$), 82.7 ($C4^{I-VII}$), 73.8, 71.0, 70.4, 70.3, 69.7, 66.3, 63.0, 61.2, 61.0 ($C2,-3,-5^{I-VII}$, $C2,-3,-4,-5,-6^{HM}$, CH₂O), 49.5 ($C6^{I-VII}$), 29.2, 29.1, 28.8, 27.9, 25.8, 25.7 (CH₂); HRMS (ES⁺): Found 3657.6952 $C_{58}H_{97}N_{21}O_{77}$ requires 3657.6895.

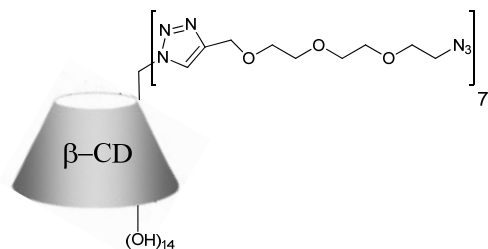
Compound 3



Compound **11** (23 mg, 111 μmol) and **13** (100 mg, 86 μmol) were dissolved in a DMF / H_2O mixture (3 / 1 mL). Copper sulfate (8 mg, 50 μmol) and sodium ascorbate (16.2 mg, 82 μmol) were added and the mixture was stirred at 70°C for 45 minutes under μW irradiation. Tetrabutylammonium iodide (2 mg, 5 μmol) and sodium iodide (28 mg, 430 μmol) were added and the mixture was heated at 80°C for 24h. Compound **10** (80 mg, 241 μmol), copper sulfate (18 mg, 113 μmol) and sodium ascorbate (36 mg, 182 μmol) were added and the mixture was stirred at 70°C for 2h under μW irradiation. The mixture was evaporated under reduced pressure and the residue purified by preparative HPLC leading to **3** (31 mg, 23%) as a white powder after lyophilisation.

$[\alpha]_D = +115$ ($c = 0.2$, H_2O); Tr = 24 min; 1H NMR (500 MHz, DMSO) $\delta = 8.03$, 8.00 (2 H, s, H_{triazol}), 5.73 (14 H, br, OH), 5.03 (1 H, br, $H-1^{HM}$), 5.00-3.80 (23 H, $H-1^{I-VII}$, OH, $H-2^{HM}$, $H-3^{HM}$), 3.80-2.80 (72 H, 7 x $H-2,-3,-4,-5,-6^{I-VII}$, $H-4,-5,-6^{HM}$, 2 x O-CH₂-triazol, 11 x CH₂), 1.46 (4 H, br, 2 x CH₂), 1.27 (6 H, br, 3 x CH₂), ^{13}C NMR (125 MHz, DMSO): $\delta = 144.0$, 143.8 ($C=CH_{\text{triazol}}$), 124.9, 124.2 ($CH=C_{\text{triazol}}$), 102.0 ($C1^{II-VII}$), 101.3 ($C1^I$), 99.7 ($C1^{HM}$), 83.4, 82.1, 81.5, 81.0 ($C4^{I-VII}$), 72.1, 71.0, 69.9, 69.5, 68.7, 66.2, 63.3, 61.3, 60.2, 60.0, 59.0 ($C2,-3,-5^{I-VII}$, $C6^{II-VII}$, $C2,-3,-4,-5,-6^{HM}$, CH₂O), 50.3, 49.3 (CH₂N, $C6^I$), 29.1, 29.0, 28.7, 25.7 (CH₂); HRMS (ES⁺): Found 1727.6538 $C_{67}H_{110}N_6O_{44}Na$ requires 1727.6609.

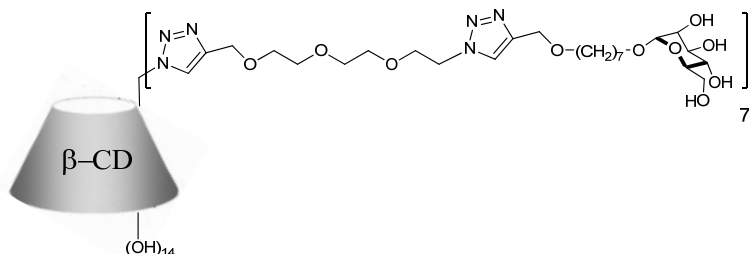
Compound 14



Compound **15** (112 mg, 423 μmol) and **12** (60 mg, 47 μmol) were dissolved in a DMF / H_2O mixture (5 / 1.6 mL). Copper sulfate (15 mg, 94 μmol) and sodium ascorbate (37 mg, 187 μmol) were added and the mixture was stirred at rt for 19h. The mixture was evaporated under reduced pressure and the residue dissolved in DMF (15 mL) with sodium azide (121 mg, 1.86 mmol). The mixture was stirred at 70°C for 36h. The mixture was evaporated under reduced pressure and the residue purified by preparative HPLC leading to **16** (21 mg, 6%) as a white powder after lyophilisation.

$[\alpha]_{\text{D}} = +84$ ($c = 0.1$, H_2O); Tr = 36 min; ^1H NMR (500 MHz, DMSO) $\delta = 7.95$ (7 H, s, $\text{H}_{\text{triazol}}$), 6.00, 5.88 (14 H, br, OH), 5.08 (7 H, br, $\text{H-1}^{\text{I-VII}}$), 4.50-4.00 (36 H, $\text{H-4}^{\text{I-VII}}$, 14 x OH, 7 x OCH_2Tri), 3.70-3.40 (126 H, $\text{H-2,-3,-4,-5,-6}^{\text{I-VII}}$, 42 x CH_2CH_2); ^{13}C NMR (125 MHz, DMSO): $\delta = 144.5$ ($\text{C}=\text{CH}_{\text{triazol}}$), 127.0 ($\text{CH}=\text{C}_{\text{triazol}}$), 102.0, 99.7 ($\text{C1}^{\text{I-VII}}$, C1^{HM}), 83.0 ($\text{C4}^{\text{I-VII}}$), 72.9, 72.1, 70.5, 70.1, 69.9, 69.7, 69.6 ($\text{C2,-3,-4,-5}^{\text{I-VII}}$, $\text{C6}^{\text{I-VII}}$, $\text{C2,-3,-4,-5,-6}^{\text{HM}}$, CH_2O), 63.5 (OCH_2Tri), 60.8 (CH_2), 50.6 (CH_2N_3); HRMS (ES $^+$): Found 942.06488 $\text{C}_{105}\text{H}_{170}\text{O}_{49}\text{N}_{42}\text{Na}_3$ requires 942.06610.

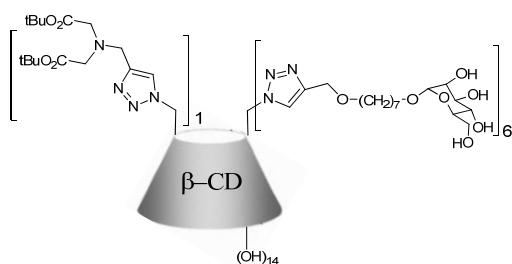
Compound 4



Compound **16** (18 mg, 6.4 μmol) and **10** (21 mg, 63 μmol) were dissolved in water (1.5 mL). Copper sulfate (4 mg, 25 μmol) and sodium ascorbate (10 mg, 50 μmol) were added and the mixture was stirred at 70°C for 45 minutes under μW irradiation. An ethylenediamine tetraacetic acid trisodium salt solution (20 mg, 50 μmol) in water (2.5 mL) was added and the mixture was stirred for 30 minutes at rt. The mixture was evaporated under reduced pressure and the residue purified by preparative HPLC leading to **17** (15 mg, 45%) as a white powder after lyophilisation.

$[\alpha]_{\text{D}} = +6$ ($c = 1$, H_2O); Tr = 21 min; ^1H NMR (500 MHz, D_2O) $\delta = 8.03$ (14 H, s, $\text{H}_{\text{triazol}}$), 5.18 (7 H, br, $\text{H}-1^{\text{HM}}$), 4.80-4.00 ($\text{H}-1^{\text{I-VII}}$, OH, $\text{H}-2^{\text{HM}}$, $\text{H}-3^{\text{HM}}$), 3.80-2.80 (209 H, $\text{H}-2,-3,-4,-5,-6$, $^{\text{I-VII}}$, 7 x $\text{H}-4,-5,-6^{\text{HM}}$, 14 x $\text{O}-\text{CH}_2\text{-triazol}$, 77 x CH_2), 1.53 (28 H, br, 14 x CH_2), 1.27 (42 H, br, 21 x CH_2), ^{13}C NMR (125 MHz, DMSO): $\delta = 144.1$, 143.8 ($\text{C}=\text{CH}_{\text{triazol}}$), 126.5, 125.3 ($\text{CH}=\text{C}_{\text{triazol}}$), 102.7, ($\text{C}1^{\text{I-VII}}$), 99.7 ($\text{C}1^{\text{HM}}$), 72.7, 70.1, 69.7, 69.5, 69.1, 68.7, 67.7, 66.7, 63.0, 62.7, 60.9 ($\text{C}2,-3,-4,-5^{\text{I-VII}}$, $\text{C}6^{\text{I-VII}}$, $\text{C}2,-3,-4,-5,-6^{\text{HM}}$, CH_2O), 50.3, 49.9 (CH_2N , $\text{C}6^{\text{I-VII}}$), 28.5, 28.3, 28.2, 25.3, 25.2 (CH_2); HRMS (ES⁺): Found 5148.4577 $\text{C}_{217}\text{H}_{360}\text{N}_{42}\text{O}_{98}\text{Na}_3$ requires 5148.4592.

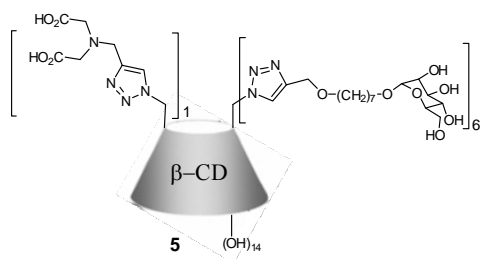
Compound 16



Compound **11** (120 mg, 91.6 μmol), **9** (182 mg, 548 μmol) and **15** (25.9 mg, 91.5 μmol) were dissolved in a dioxane / water mixture (7.5 / 1.5 mL). Copper sulfate (29 mg, 182 μmol) and sodium ascorbate (72 mg, 363 μmol) were added and the mixture was stirred at 90°C for 1h30 under μW irradiation. Ethylenediamine tetraacetic acid trisodium salt (150 mg, 50 μmol) was added and the mixture was stirred for 30 minutes at rt. The mixture was evaporated under reduced pressure and the residue purified by preparative HPLC leading to **2** (78 mg, 22%), **17** (54 mg, 16%), and **18** (21 mg, 6%, Tr = 38 min), as white powders after lyophilisation.

$[\alpha]_D = +21$ ($c = 0.3$, H_2O); Tr = 36 min; ^1H NMR (500 MHz, DMSO) $\delta = 7.95, 7.90, 7.86, 7.71$ (7 H, s, $\text{H}_{\text{triazol}}$), 6.01, 5.89 (12 H, br, OH), 5.05 (7H, s, $\text{H-1}^{\text{I-VII}}$), 4.65-4.00 ($\text{H-4}^{\text{I-VII}}$, 3 x CH_2 , OH, 6 x OCH_2Tri , 6 x H-1^{HM}), 3.60-3.20 (99 H, br, $\text{H-2,-3,-5,-6}^{\text{I-VII}}$, 6 x $\text{H-2,-3,-4,-5,-6}^{\text{HM}}$, 14 x CH_2), 1.50-1.20 (78 H, m, 30 x CH_2 , 6 x CH_3), ^{13}C NMR (125 MHz, DMSO): $\delta = 170.0$ (CO), 144.8 ($\text{C}=\text{CH}_{\text{triazol}}$), 125.3 ($\text{CH}=\text{C}_{\text{triazol}}$), 101.7 ($\text{C1}^{\text{I-VII}}$), 99.8 (C1^{HM}), 82.8, 80.3 ($\text{C4}^{\text{I-VII}}$), 73.9, 71.1, 70.4, 69.7, 66.2, 63.0, 61.3 ($\text{C2,-3,-5}^{\text{I-VII}}$, $\text{C2,-3,-4,-5,-6}^{\text{HM}}$, CH_2), 54.5, 49.5 ($\text{C6}^{\text{I-VII}}$), 29.0, 28.8 (CH_2), 27.8 (CH_3), 25.7 (CH_2); HRMS (ES⁺): Found 3608.6622 $\text{C}_{153}\text{H}_{254}\text{N}_{22}\text{O}_{74}\text{Na}$ requires 3608.6843.

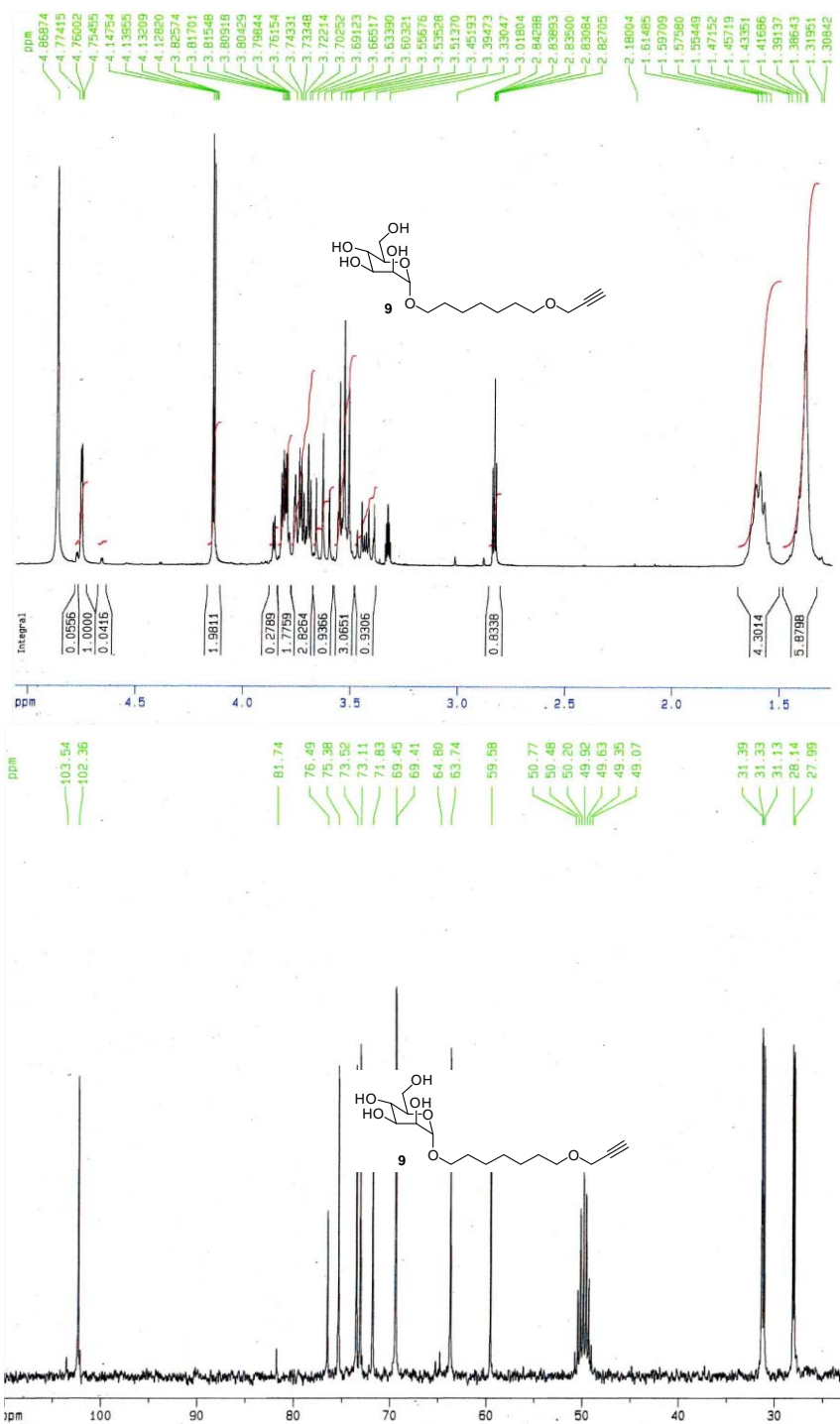
Compound **5**

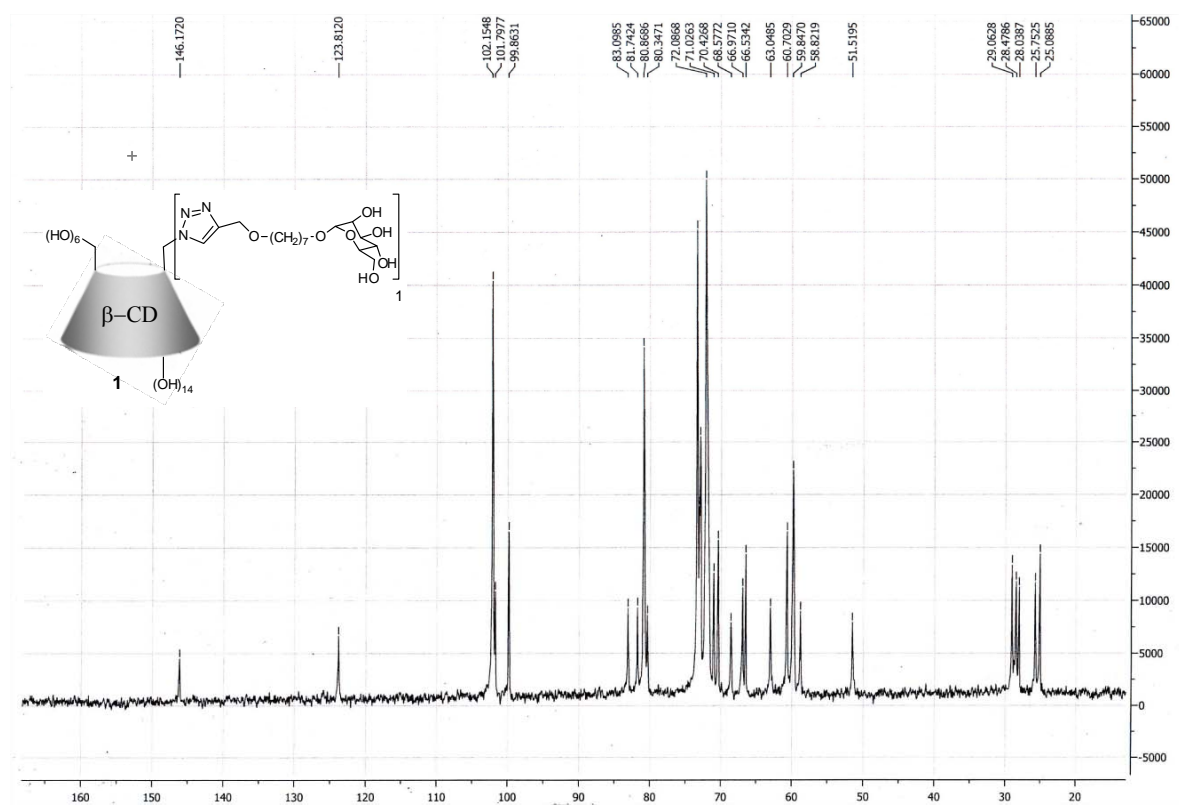
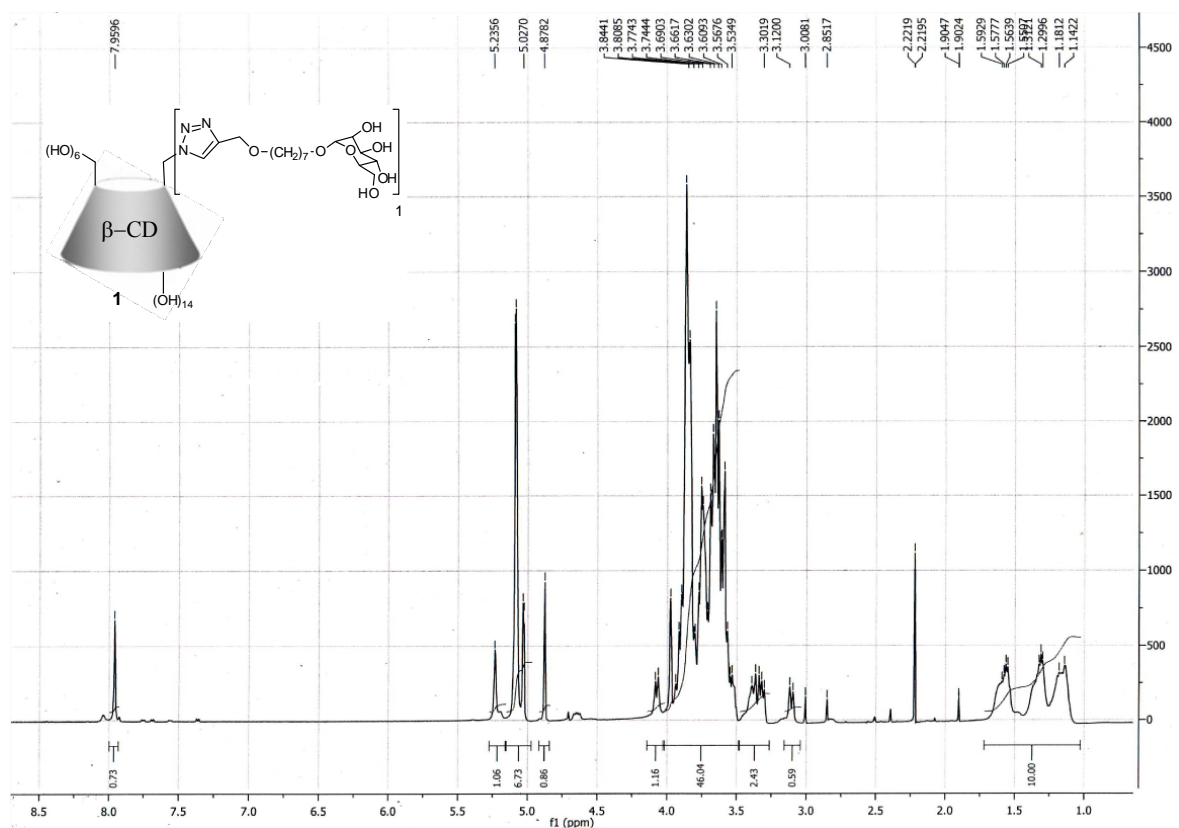


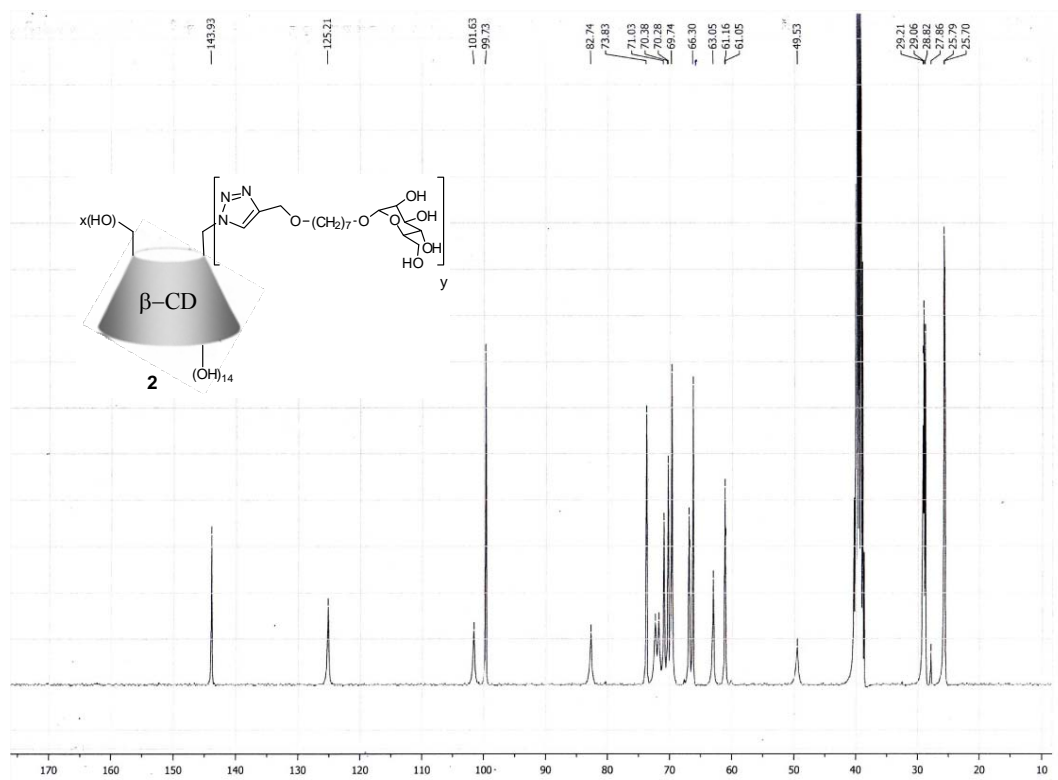
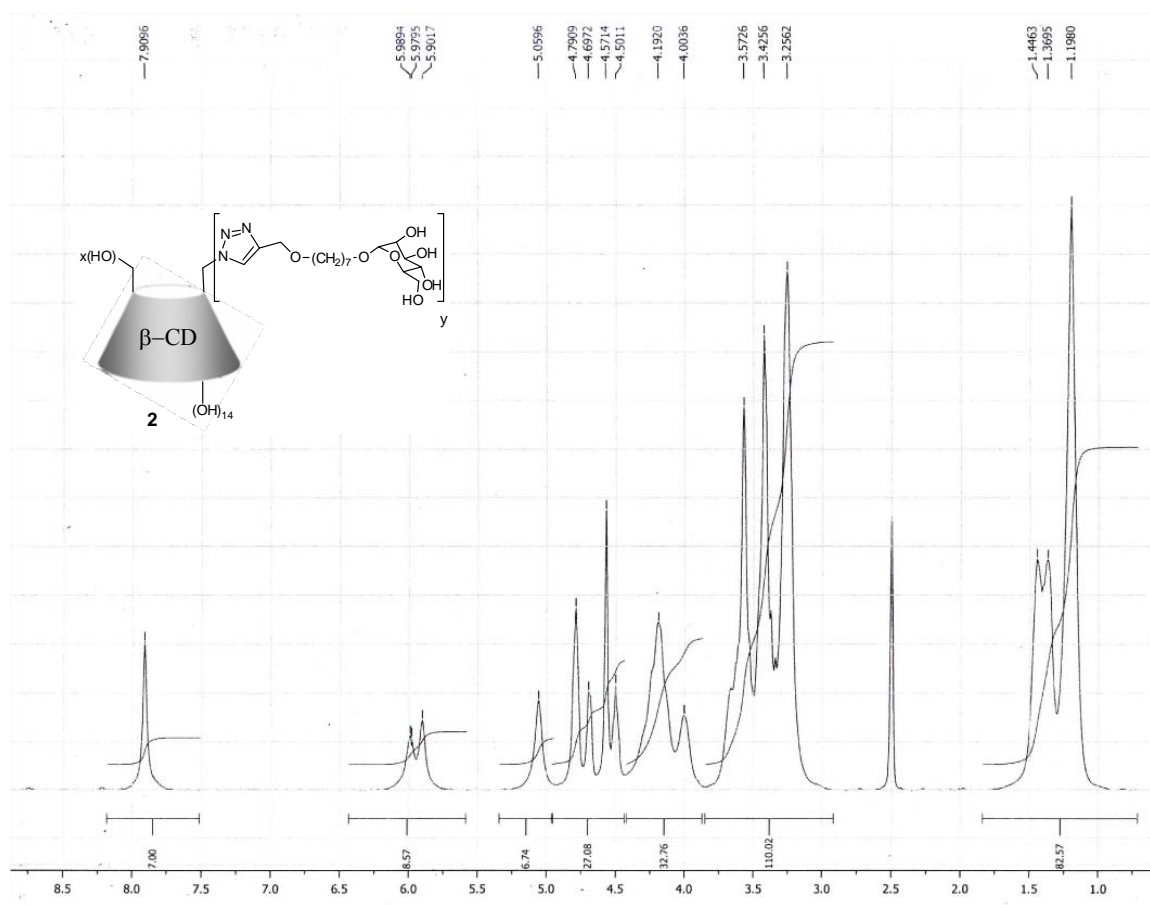
Compound **16** (10 mg, 2.8 μmol) was dissolved in pure TFA (2 mL) and the solution was stirred at rt. for 4h. The solvent was removed under reduced pressure and the residue was lyophilized to lead to **5** quantitatively.

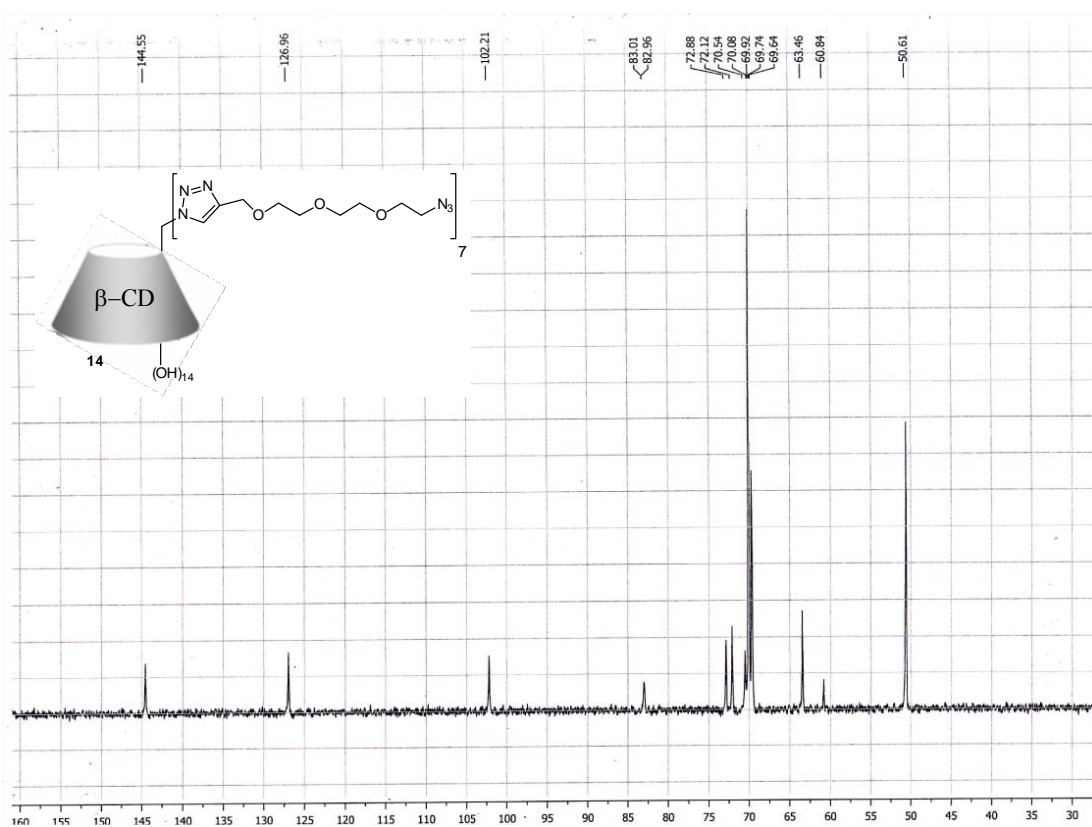
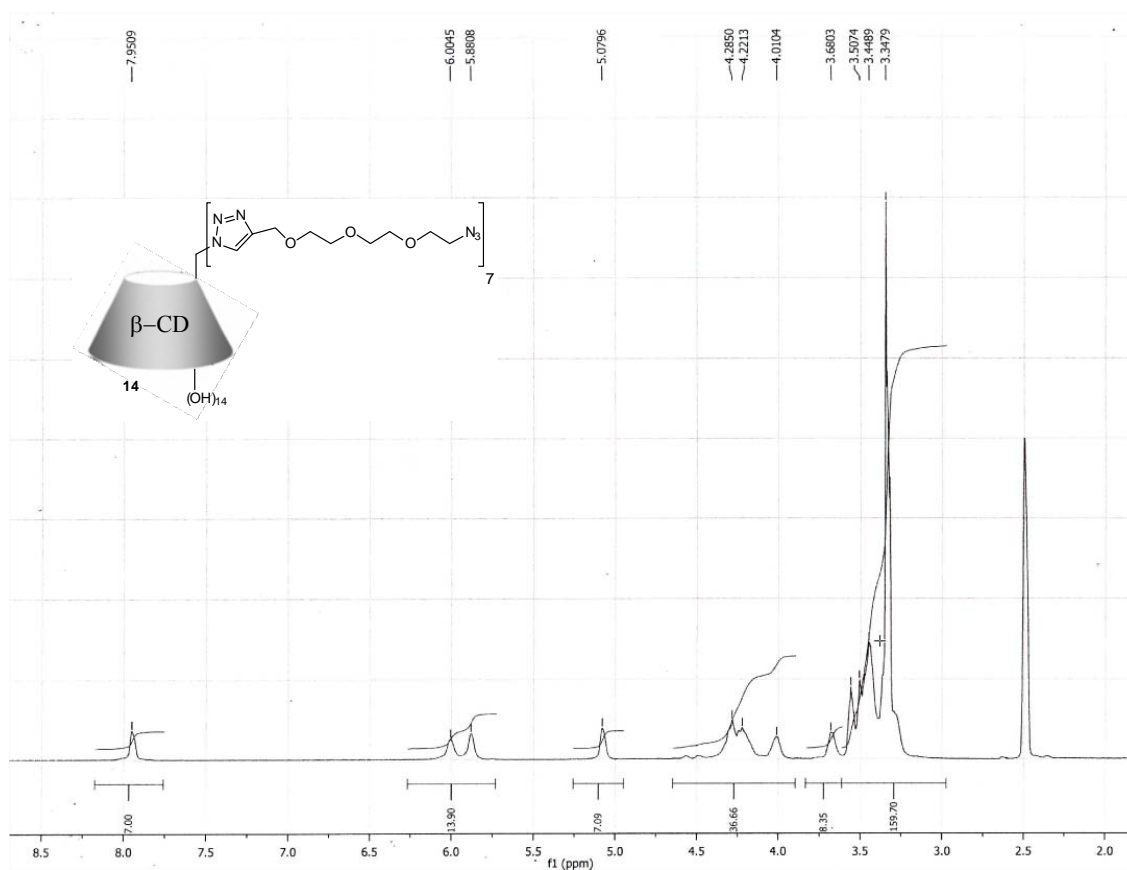
$[\alpha]_{\text{D}} = +23$ ($c = 0.6$, H_2O); ^1H NMR (500 MHz, DMSO) $\delta = 8.01, 7.94, 7.91, 7.85$ (7 H, s, $\text{H}_{\text{triazol}}$), 5.92 (2 H, br, OH), 5.07 (7 H, s, $\text{H-1}^{\text{I-VII}}$), 4.65-4.00 ($\text{H-4}^{\text{I-VII}}$, 3 x CH_2 , OH, 6 x OCH_2Tri , 6 x H-1^{HM}), 3.60-3.20 (99 H, br, $\text{H-2,-3,-5,-6}^{\text{I-VII}}$, 6 x $\text{H-2,-3,-4,-5,-6}^{\text{HM}}$, 14 x CH_2), 1.45-1.20 (60 H, m, 30 x CH_2), ^{13}C NMR (125 MHz, DMSO): $\delta = 171.4$ (CO), 143.9 ($\text{C}=\text{CH}_{\text{triazol}}$), 125.3 ($\text{CH}=\text{C}_{\text{triazol}}$), 101.7 ($\text{C1}^{\text{I-VII}}$), 99.8 (C1^{HM}), 82.8 ($\text{C4}^{\text{I-VII}}$), 73.9, 71.1, 70.4, 69.7, 66.3, 63.1, 61.3 ($\text{C2,-3,-5}^{\text{I-VII}}$, $\text{C2,-3,-4,-5,-6}^{\text{HM}}$, CH_2), 53.4, 49.5, 48.2 ($\text{C6}^{\text{I-VII}}$), 29.2, 29.0, 28.8, 25.8, 25.7 (CH_2); HRMS (ES⁺): Found 3472.5642 $\text{C}_{145}\text{H}_{236}\text{N}_{22}\text{O}_{74}$ requires 3472.562.

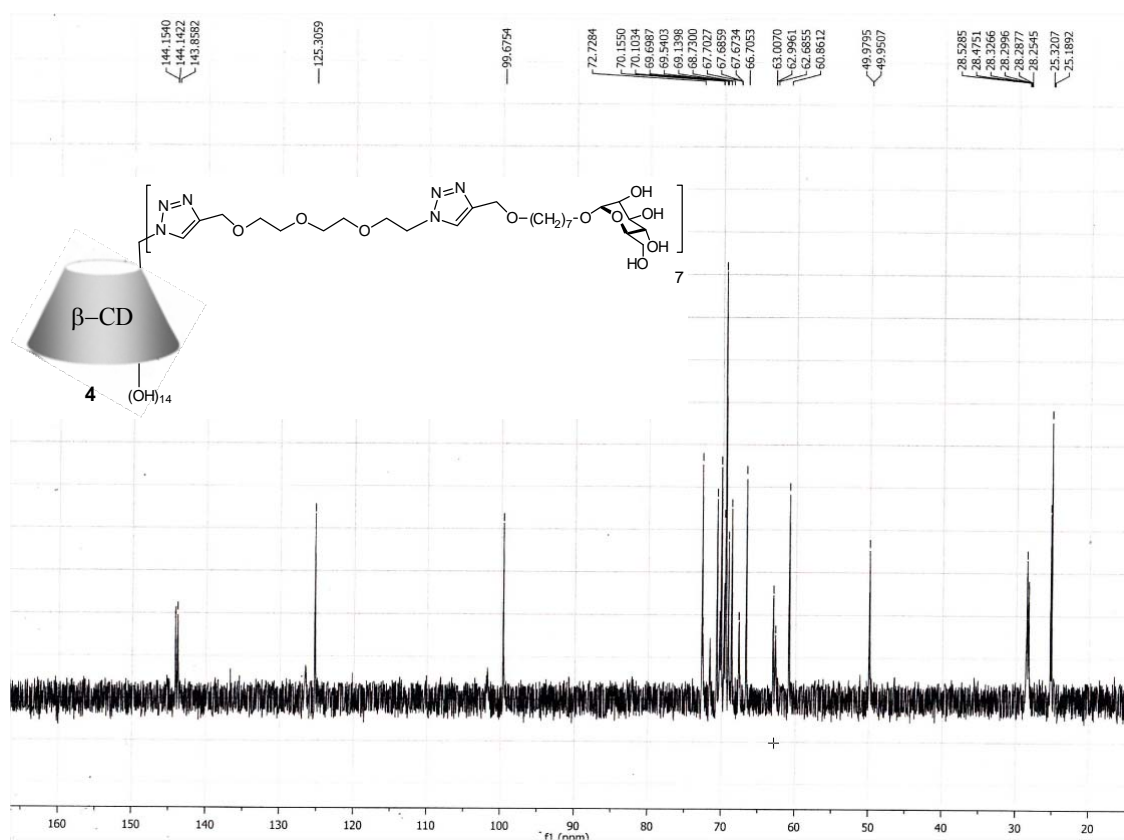
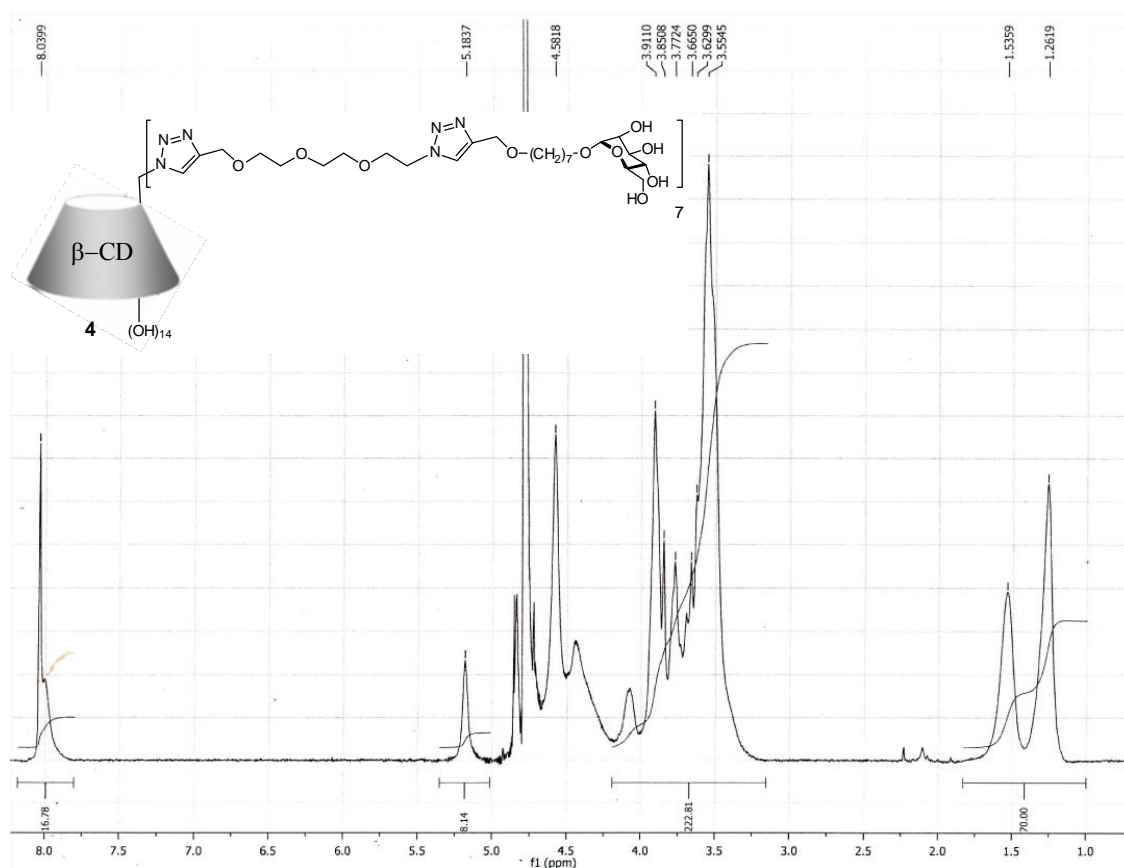
NMR spectra of synthetic products

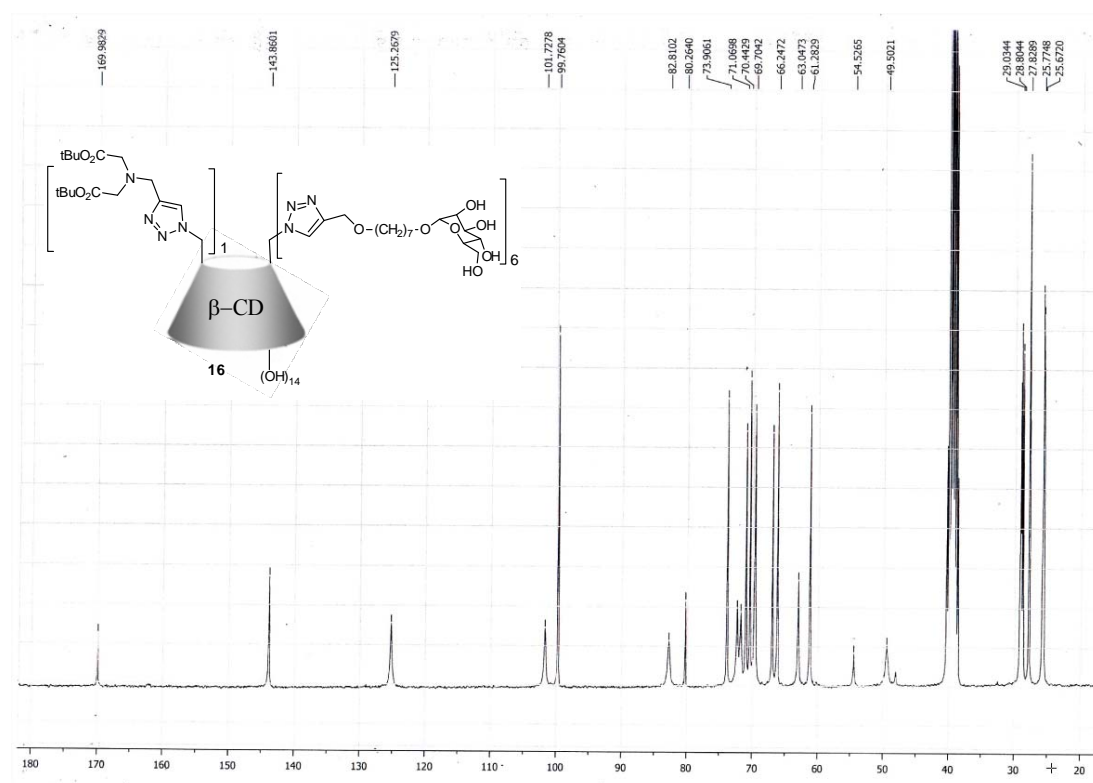
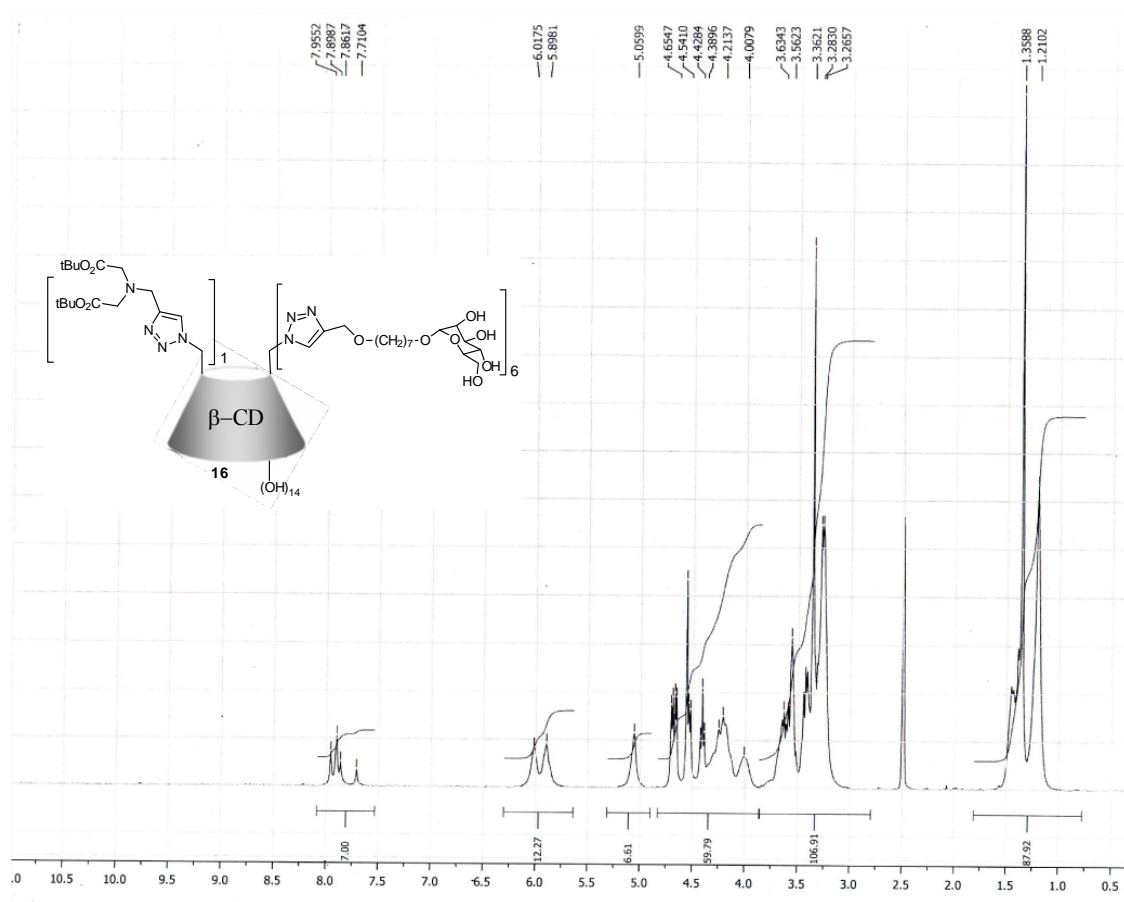


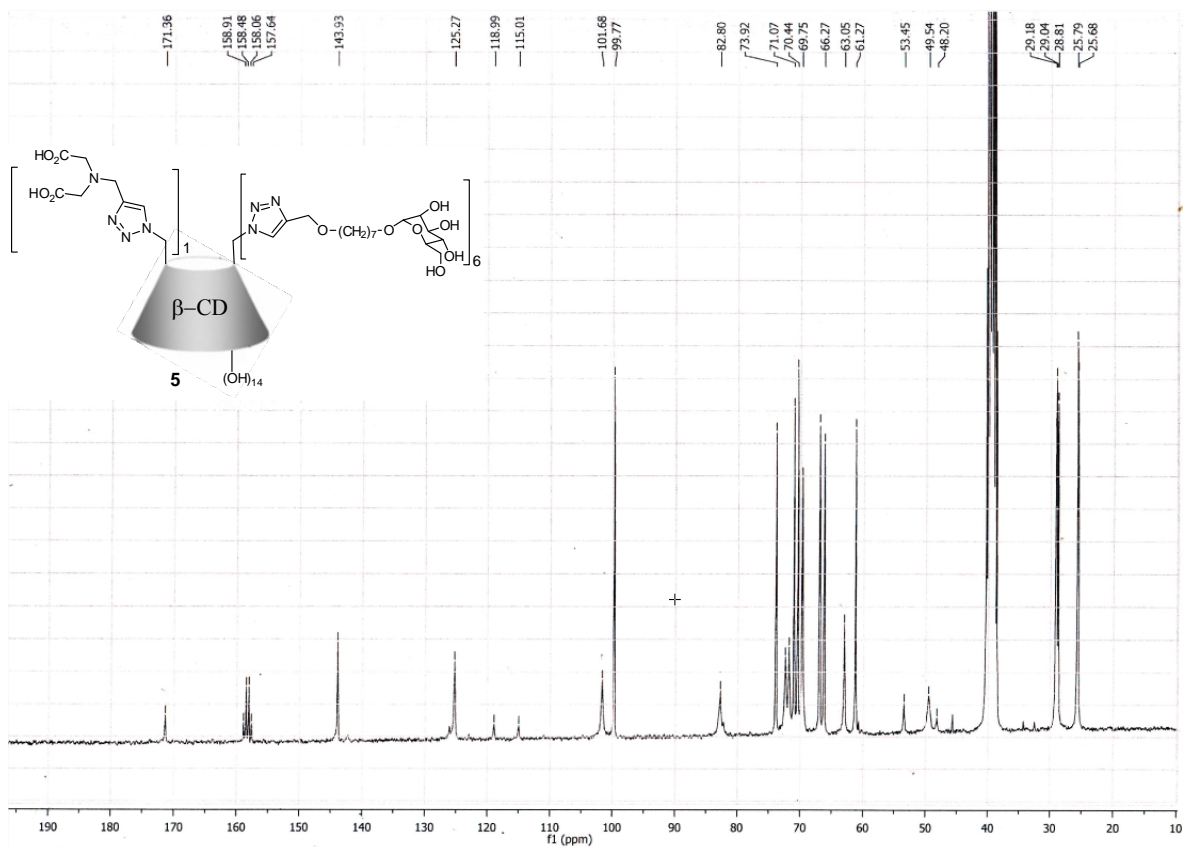
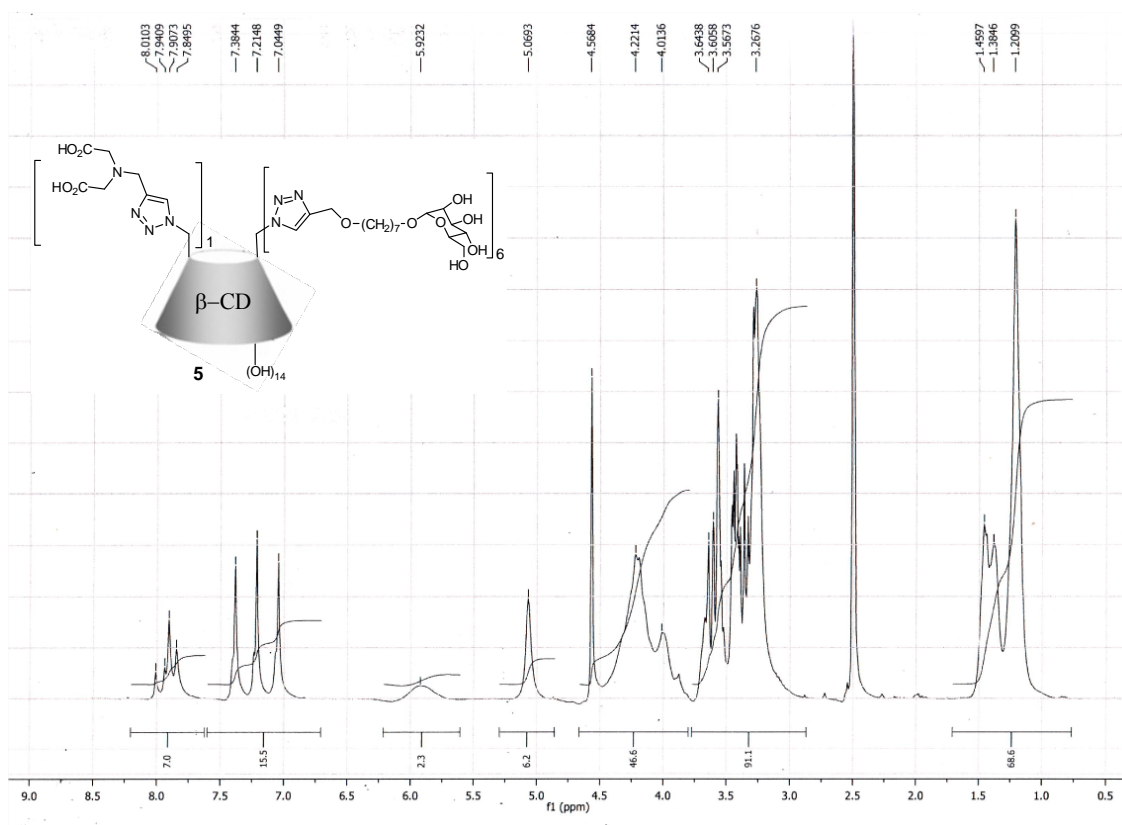












Procedure and data for isothermal titration calorimetry (ITC): The FimH adhesin lectin domain was expressed and purified as previously described [Almant, M.; Moreau, V.; Kovensky, J.; Bouckaert, J.; Gouin S.G. *Chem. Eur. J.* **2011**, *17*, 10029-38] and finally dialysed against 20 mM HEPES pH 7.4 with 150 mM NaCl. The last change of dialysis buffer was filter-sterilized and kept as buffer to dilute FimH and compounds for the calorimetry. A VP-ITC (Microcal) and ITC-200 (GE Healthcare) were used both for direct and reverse titrations. Using VP-ITC, always 280 μ l was injected into the 1.4253 ml measurement cell. To obtain fine details for distinct heat signals originating from ligand release and ligand binding respectively for the monovalent cyclodextrins, we used an ITC-200 instrument (GE Healthcare) with a 40 μ l syringe volume and a 200 μ l cell volume, and the frequency of recording was set to 1/second. Respective concentrations and molar ratios in needle and cell, injection volumes and time intervals between injections were varied to obtain 1) inflection and saturation about half-way the experiment 2) sufficient heat production per injection to allow good peak integration, and 3) sufficient time between the injections to allow a return to equilibrium. The concentrations used in every ITC experiment are presented on the curves. Stirring speed of the needle was always 307 rpm. Fitting was performed using the Origin software using the equations for one set of binding sites.

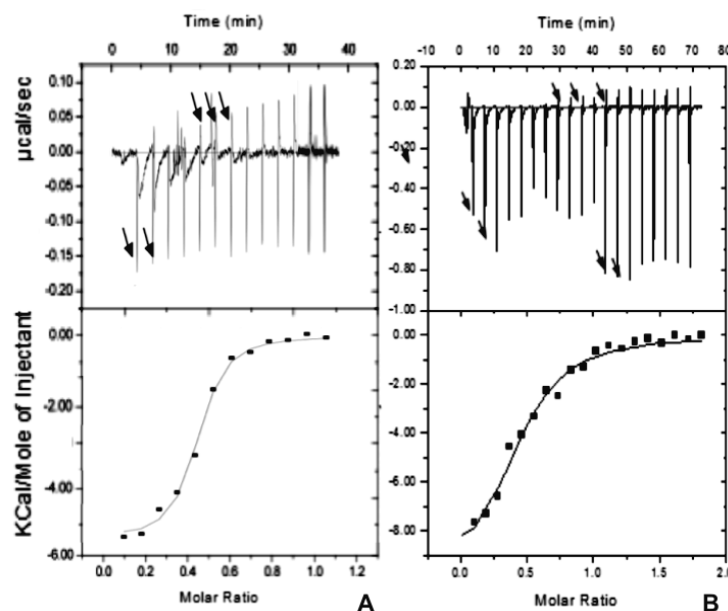
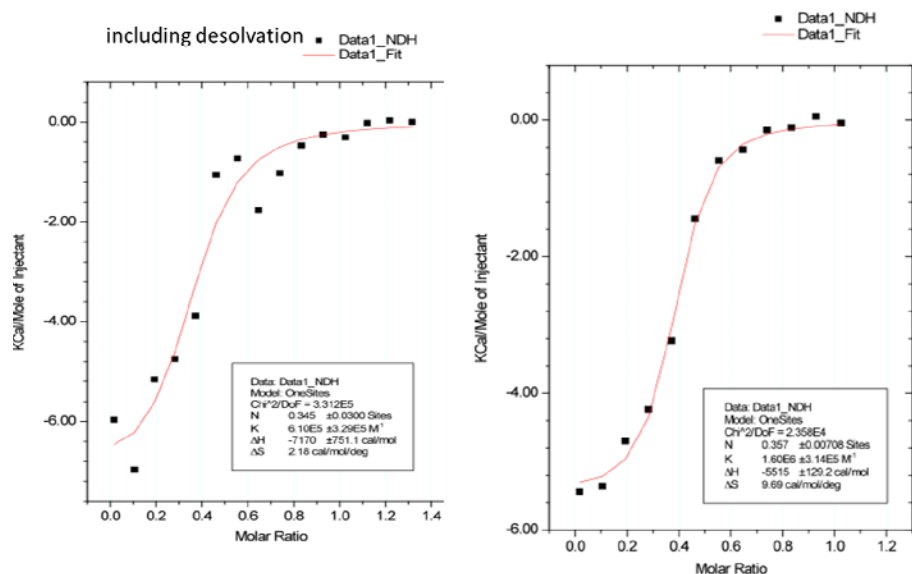


Figure S1. Direct titrations of **1** (A) and **3** (B) to FimH show narrow exothermic peaks (arrows, low) upon each injection, immediately followed by narrow endothermic signals (arrows, up) once FimH is saturated. The elution peaks were filtered out to obtain the fit to the data points in the lower panel (see also Figures S2).

FimH:1

Processed to filter out only binding:



FimH:3

no filtering → filtering for only binding

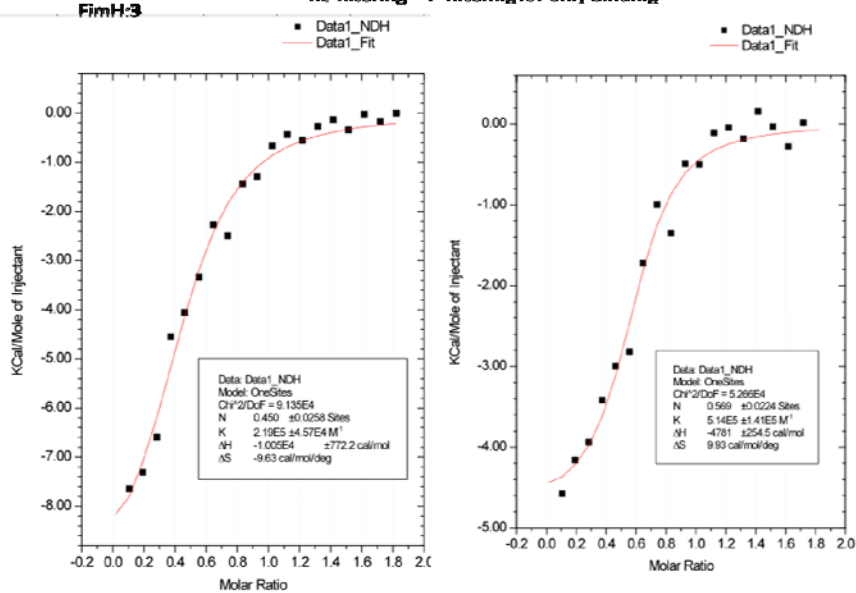


Figure S2. Representative ITC curves for the direct titrations of **1** and **3** respectively, with (left) and without (right) inclusion of the elution heat peak. In each case, 400 μ M of **1** or **2** were titrated into 45.15 μ M FimH in the measurement cell. In both cases, the fit (evaluated by χ^2) was substantially improved upon filtering of the heat peaks, to include only those the heat peaks that are related to complex formation, and to exclude the narrow heat peaks that are possibly due elution of the heptyl (ligand **1**) and heptyl plus polyethylene glycol linker (**3**) from the inner cavity of the cyclodextrin cone.

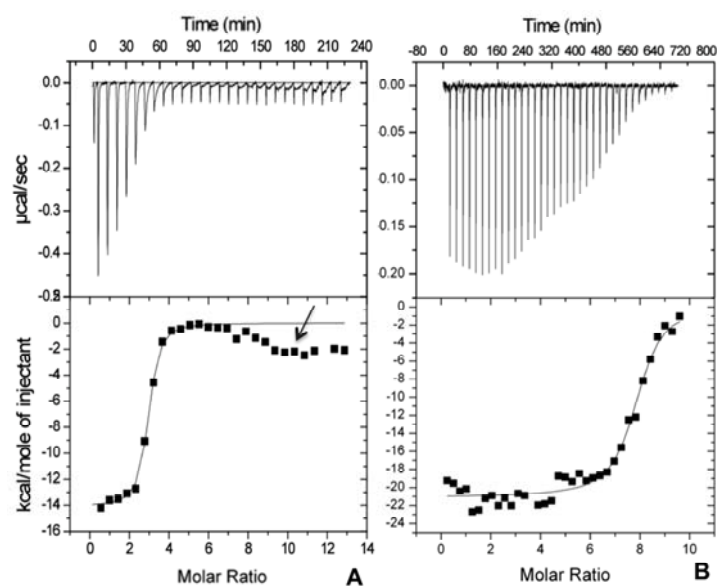


Figure S3: Reverse ITC with compound **2** and **4**.

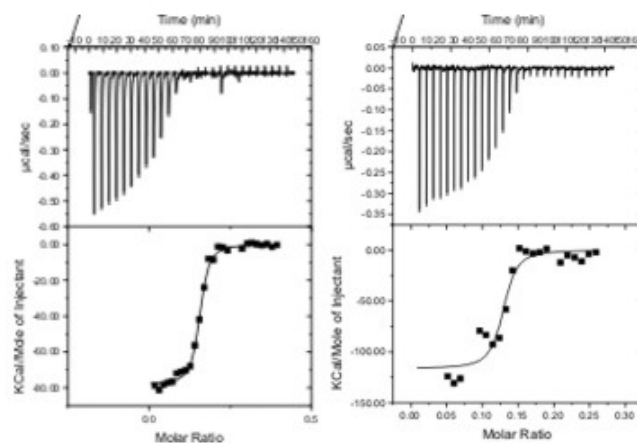


Figure S4. Direct titrations of 30 μM of ligand **2** into 20 μM of the FimH lectin domain (left) and of 12 μM of ligand **4** into 10 μM FimH.

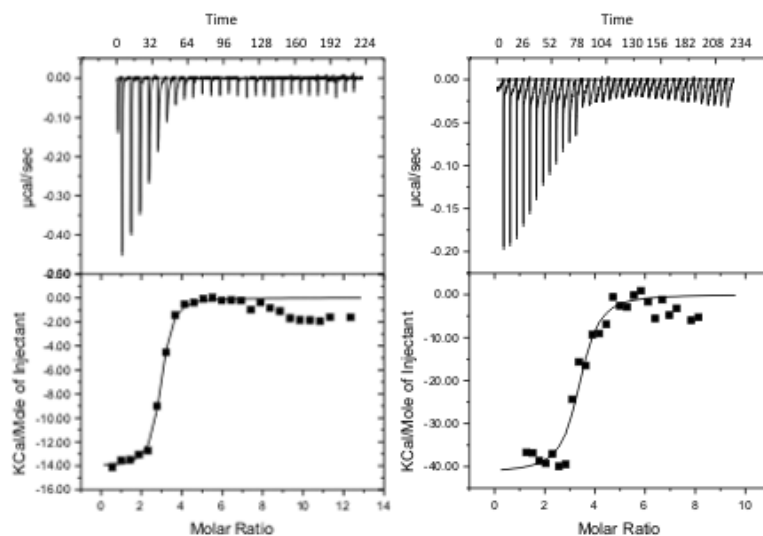


Figure S5. Repeated reverse titrations of the FimH lectin domain at 44,51 μM into a solution of 1 μM of **2** in the ITC measurement cell. Beyond a molar ratio of 6, an exothermic dump in the baseline is observed, indicative of secondary interaction events. The SAXS and DLS experiments (Figure S7 and Table S1) indicate that these secondary interaction events are weak, reversible protein-protein interactions.

Small angle X-ray solution scattering

SAXS data were collected on the EMBL-X33 beamline at the DORIS III storage ring (DESY, Hamburg, Germany). Preparative experiments on the FimH lectin domain alone have been done before at beamline SWING at SOLEIL. Samples of FimH were dialyzed against 25 mM HEPES, 150 mM NaCl, 0.5 mM EDTA and 5 mM DTT. To make the FimH-cyclodextrin complexes, the proteins were mixed with the ligands **1** and **2**, in 1:1 and 7:1 FimH:β-CD molar concentration ratios, respectively. The samples were then concentrated, to generate the highest concentration of the FimH-β-CD complex. The eluent of the centricon used for concentrating the protein was used as the blank for SAXS experiments with the particular FimH: β-CD complex. In addition the same eluent was used to generate a dilution series of each complex. Immediately prior to DLS and SAXS measurements, the protein and complex solutions were centrifuged for 1 hour at 4°C in a table top centrifuge to remove possible aggregates, and the concentration of samples was again measured, applying the conversion of OD_{280nm} of 1.532 for 1 mg/ml FimH. SAXS curves were measured at 10°C over the range of momentum transfer $0.008 \text{ \AA}^{-1} < q < 0.60 \text{ \AA}^{-1}$ (where $q = 4\pi \sin(\theta)/\lambda$; 2θ is the scattering angle and $\lambda=1.5 \text{ \AA}$ is the X-ray wavelength). For data collection, 2-minute exposures split into 15-second collection windows were used to minimise radiation damage. The scattering curves were examined and processed using PRIMUS.

A model of FimH bound to the heptavalent compound based on the SAXS data, was generated by first generating manually a trimeric model using MASHA. Rigid body refinement was then performed on this initial structure using CORAL. A number of distance constraints were applied during the refinement process to ensure that the mannose receptor-binding sites remained arranged pointing to the β-CD cone.

The I_0 value for the lowest concentration of the (FimH)₃:**2** complex is close to the value at infinite dilution, therefore we used this curve to generate a model of the complex. Initial attempts to build a model by *ab initio* methods failed. Therefore we employed a strategy first using manual building with available crystal structures, followed by a round of rigid body refinement. The trimeric FimH:**2** SAXS model indicates that the tyrosine gate (Tyr48 and Tyr137) of FimH is directed towards the β-CD for all 3 FimH molecules and fits very well (χ^2 from CRY SOL 0.92) with the 3:1 stoichiometry of the FimH:**2** found in reverse isothermic calorimetry titrations of the FimH lectin domain into the measurement cell containing β-CD **2**.

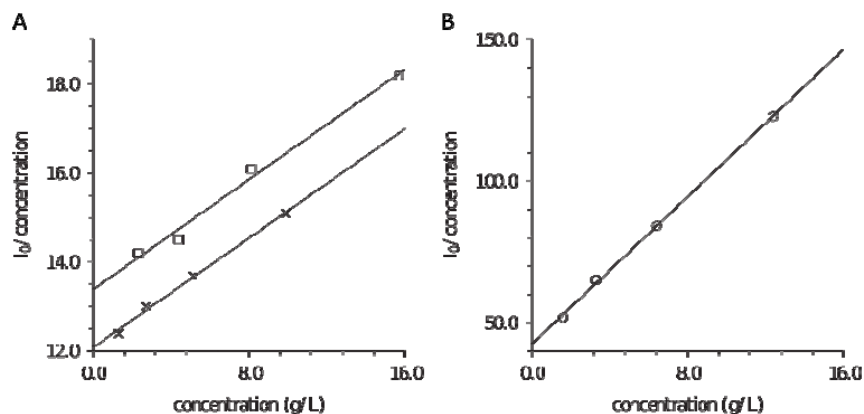


Figure S6. The SAXS scattering intensity at I_0 is affected by sample concentration. Plots of I_0 values versus sample concentration for ligand-free FimH (panel A, crosses), bound to the monovalent ligand **1** (panel A, squares) and bound to heptavalent ligand **2** (panel B, circles) show increasing I_0 for increasing concentrations of FimH. The intensity at I_0 was determined by Guinier analysis of the scaled data by linear least squares fitting through the data points using AUTORG (Figure S8).

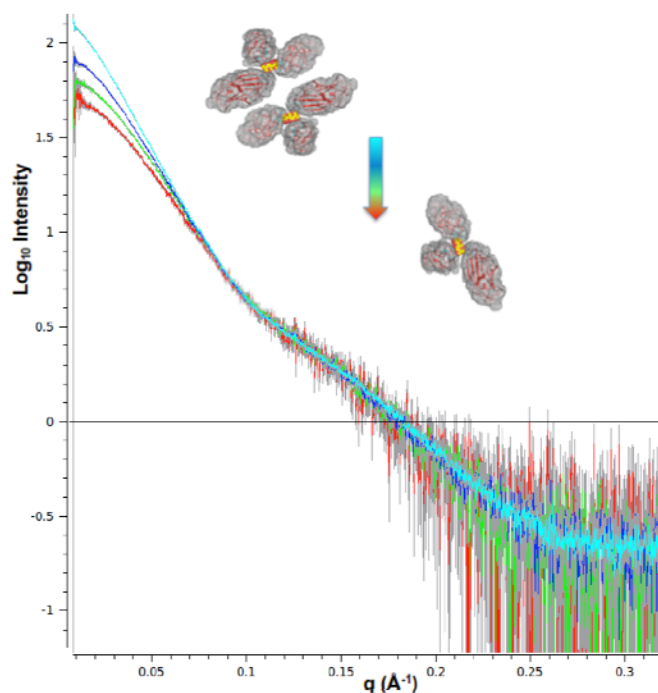


Figure S7 Concentration-dependent increase in the size of the FimH-2 complex, showing possible higher order oligomer formation based on the inter-trimer interactions. Two-fold dilutions in the same buffer of 12.4 g/l (cyan) to 6.4 g/l (blue), 3.3 g/l (green) and 1.6 g/l (red) demonstrate that more of a higher-order species exists at higher concentrations that readily dissociates, upon dilution, towards the stable (FimH)₃:2 trimeric complex that is observed in reverse isothermal titrations (Figure S5).

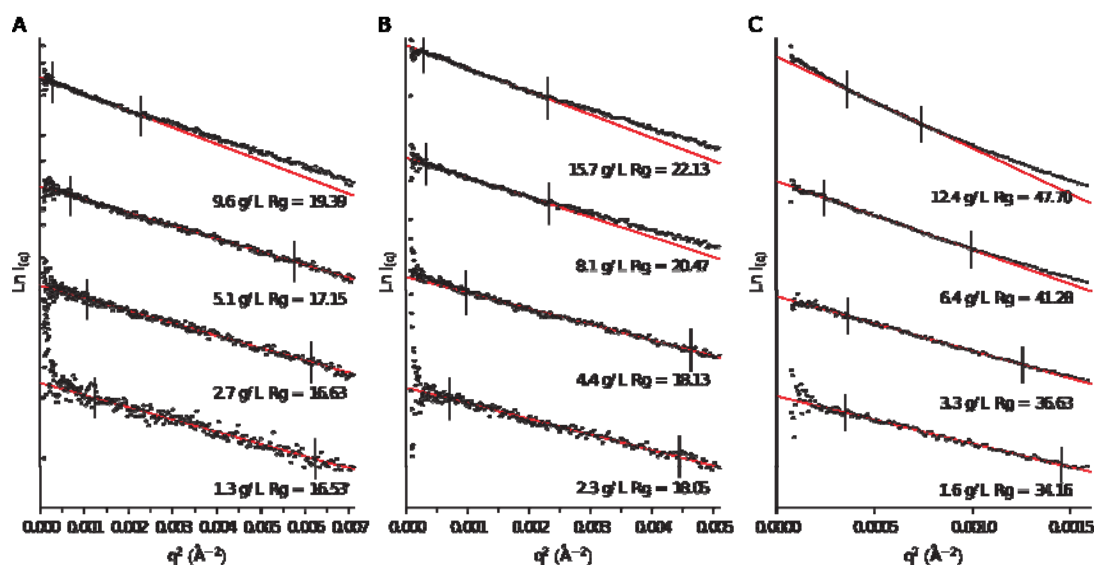


Figure S8. Guinier analysis of the SAXS curves of FimH alone (A), FimH premixed with **1** (B) and FimH premixed with **2** (C). For each sample SAXS data were measured at four different concentrations. Guinier plots were generated using PyXPlot (<http://www.pyxplot.org.uk>) where each curve is offset by a factor of 2 to the curve below it. The vertical lines on each plot correspond to the lower and upper limits of the q^2 values, predetermined using AUTORG ; Petoukhov, M.V.; Konarev, P.V.; Kikhney, A.G.; Svergun, D.I. *J. Appl. Cryst.* **2007**, *40*, s223–8), between which linear least squares fitting was performed. The reported R_g values correspond to the slope of the fitted line (Table S1).

Dynamic light scattering

Dynamic light scattering data (DLS) have been collected on apo-FimH, the FimH in complex with **1** complex and the FimH in complex with **2**, on a Malvern nanoDLS instrument. The samples were identical to those used to collect SAXS data, except that here all dilutions were made in PBS. All samples were subjected to centrifugation at 40.000g during 60 min. The mass distribution molecular weight calculations (column Complex (kDa) at the lowest concentration confirm the theoretical molecular weight for apo-FimH, a 1:1 complex of FimH:**1** (hereafter called FimH:**1**) and a 3:1 complex for FimH:**2** (hereafter called (FimH)₃:**2**). The basic protein-carbohydrate complexes as found in ITC for the binding of the FimH lectin domain to the *n*-heptyl α -D-mannose-derivatized β -CDs (Figures S1, S3), are thus confirmed using both light and X-ray scattering methods.

DLS					Cummulant fitting			Intensity distribution (ID)			Mass distri. (MD)		Complex	Oligomer	SAXS		
APO	MM theo	16,907.90			(nm)	(nm)		(nm)	(nm)	kDa	distri.	APO	(nm)	(kDa)			
kcps	mg/ml	Z (r.nm)	Std Dev	PDI	R mean	Std Dev	%PD Int	R mode	Std Dev	MD MW	% dimer	mg/ml	Rg	MW			
1590	14.42	2.64	0.11		0.2	2.77	0.84	30.50	1.81	0.66	20.4	67.0	9.9	1.94	17		
													5.1	1.71	15		
426	3.61	2.19	0	0.06	2.35	0.66	28.10	1.81	0.50	15.0	50.0	2.7	1.66	14			
													1.3	1.65	14		
cpd 1	MM theo	18,400.00											cpd 1				
kcps	mg/ml	Z (r.nm)	std	PDI	R mean	Std Dev	%PD Int	R mode	Std Dev	MD MW	% dimer	mg/ml	Rg	MM			
2500	15.30	2.84	0.04	0.16	3.01	0.89	29.40	2.09	0.71	25.9	57	15.7	2.21	23			
												8.1	2.05	19			
977	3.83	3	0.02	0.25	2.96	0.99	33.50	1.81	0.73	21.2	57	4.4	1.81	17			
354	1.91	2.59	0.07	0.26	2.47	0.74	29.80	1.81	0.58	15.9	60	2.1	1.80	16			
cpd 2	MM theo trimer	54.360,50											cpd 2				
kcps	mg/ml	Z (r.nm)	std	PDI	R mean	Std Dev	%PD Int	R mode	Std Dev	MD MW	% dimer	mg/ml	Rg	MM			
4963	10.15	5.4	0.02	0.11	6.09	2.18	35.90	3.77	1.52	105.0	41	12.4	4.77	117			
												6.4	4.13	83			
1143	2.54	4.2	0.01	0.11	4.68	1.54	33.00	3.25	1.15	63.3	79	3.3	3.66	64			
588	1.27	4.04	0.03	0.08	4.41	1.34	31.00	2.81	1.06	57.8	72	1.6	3.41	57			

Table S1: DLS and SAXS data for the apo-FimH and complexes of FimH with β -CDs **1** or **2**. Theoretical molecular weights (MW) of the complexes are indicated. (1) Both DLS (R mode = radius of hydration in the modal distribution) and MD = mass distribution) and SAXS (Rg = radius of gyration) indicate monomers for apo-FimH and the FimH:**1** complex and a trimer for FimH:**2**. The (FimH)₃:**2** trimer found by ITC is thus confirmed. (2) Both in SAXS and DLS experiments, Rg and MW are increasing with increasing concentrations, however there were never two peaks observed in DLS measurements. Similarly, in ITC, secondary interactions with exothermic character take place above a molar ratio of 6 FimH molecules, which could agree with the formation of dimers of trimers for (FimH)₃:**2** (see Figures S5, S7).

Already for the apo-FimH protein, a clear concentration dependence of association is observed. We can therefore assume we have a weak self-association that does not result in a new assembly (as suggested by the SAXS at higher q). A same protein-protein association appears to happen for the (FimH)₃:**2** complex, where in this case each protomer of the trimer has an equivalent propensity to interact with one another. The estimate of the distribution of monomers (apo-FimH, FimH:**1** complex and (FimH)₃:**2** complex) vs higher order aggregates such as dimers of those monomers was performed using the mass distribution of DLS. The column on oligomer distribution predicts the percentage of dimer in case only monomer and dimer (of the basic monomer) would be formed. There were never two peaks observed in DLS measurements for the apo-FimH and complexes of FimH with β -CDs **1** or **2**.

Epifluorescence microscopy: UTI189 *E. coli* strains were grown statically overnight in LB at 37°C, washed (3 times) and diluted in PBS (137mM NaCl, 2.7mM KCl, 10mM Na₂HPO₄, 1.76mM K₂HPO₄, pH 7.4) to an OD_{600nm} = 1. 100 µl of glycoconjugate-agglutinated *E. coli* were washed in 1 ml PBS, resuspended in 200 µl 0.1% acridin orange and left at room temperature for 2.5 hours. The bacterial cells were washed again in 1 ml PBS to remove unbound acridin orange. A microscope glass was rinsed with 100% EtOH and next dried at the air. A 5 µl cell suspension was put on the microscope glass, dried at the air and visualised using a laser with excitation wavelength of 408 nm.

MATERIALS AND METHODS FOR DYNAMIC IMAGING AND PHARMACODISTRIBUTIONS

Labelling of **5**

Labelling of **5** with $[^{99m}\text{Tc}(\text{CO})_3]^+$ was performed in a glass vial under nitrogen, 200 μl of 1×10^{-4} M aqueous solution of compound **5** was added to 1.2 mL of $[^{99m}\text{Tc}(\text{OH}_2)_3(\text{CO})_3]^+$ in NaCl 0.9% (pH = 7) prepared using an Isolink kit (Mallinckrodt Medical, Petten, The Netherlands) and the mixture was incubated for 45 min at 100 °C. The resulting complex was analyzed by RP-HPLC (Column: Analytical, C4 column 214TP53, 0.32 x 25 cm, Grace Vydac, Flow: 0.5 mL/min; γ detection) (R_t = 12 min) and the labelling yield was higher than 95%. The eluent was 0.1% TFA in H_2O (solvent A) and CH_3CN (solvent B). For the analytical control the method was as follows: 0-3 min., 0% B; 3-3.1 min., 0-25% B; 3.1-9 min., 25-100% B; 9-20 min., 100% solvent B.

Dynamic imaging

Injection of tracer compound **5** with activities of 2,014 mCi, 1,644 mCi and 1,554 mCi, respectively, in the eye vein of three C3HHeN mice was done to allow real time imaging in C3H/HeN. Image acquisition was performed with a left lateral positioning total-body pinhole SPECT scan using a dual-head γ -camera, mounted with 2 multi-pinhole collimators (3 pinholes of 1.5 mm in each collimator, 200-mm focal length, 80-mm radius of rotation, e.cam180; Siemens Medical Solutions), for 60 images of 1 minute. On both modalities, the animals were imaged in the same animal holder, which included 2 plastic discs, each containing three ^{57}Co (3.7 MBq) sources (Canberra-Packard). A micro-CT scan was performed using a dual-source CT scanner with 60 kV and 615 mA at a resolution of 83 μm . The six ^{57}Co sources were detected on both micro-CT and pinhole SPECT and used for alignment of CT and SPECT images. Image reconstruction was performed using filtered back-projection (Nrecon; Skyscan). Image processing took into account a sensitivity correction for the pinhole opening. Analyses of total body, liver, kidneys, bladder and heart outputs of distributions the bifunctional CD 20 in the regions of interest (ROI) expressed in % of injected activity (%IA).

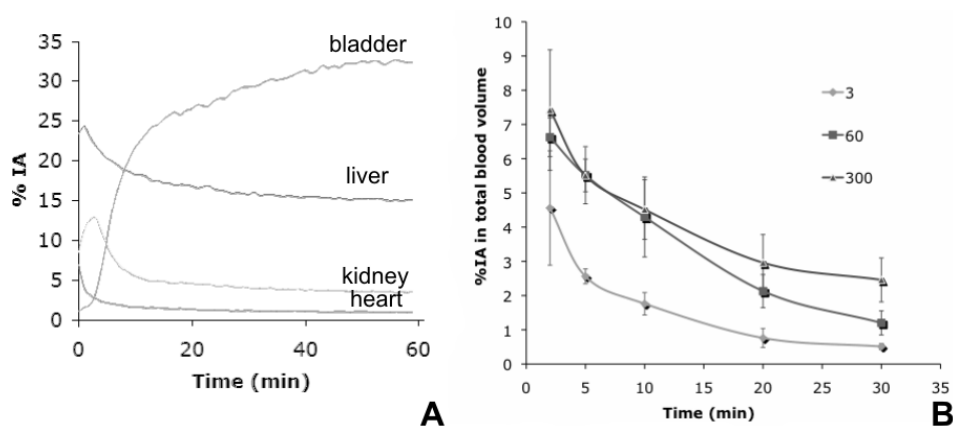


Figure S9 (A) Distribution of **5** in the heart, liver, kidney and bladder by processing of dynamic images (the 2 other mice in the supplementary information). **B** The blood curves (3, 60 or 300 µg) show a rapid clearance of **5** through the kidneys into the bladder.

Distribution by dissections and blood curves

Quantitative samplings of **5** was performed using three different doses (3 µg, 60 µg and 300 µg), between 2' and 30' post -injection, with for each time point four mice. Blood curves were composed over this time period. Dissections were also performed at the later time points of 1h, 3h, 6h and 24h for the lowest dose. Dissection allowed measurement of activity per gram (% of the injected activity) in kidney, liver and bladder. These time points were chosen to cover the pathogenic cycle of UTI89 in the C3H/HeN mouse: 0-6 hours adhesion, invasion and early IBC (intracellular bacterial communities) formation, 6-12h (maturation into mid-IBCs), from 16h and on: fluxing out of bladder wall, spreading in filamentous shape into the bladder lumen and re-initiation of the IBC cascade [Justice S.; Hung C., Theriot J.; Fletcher D.; Anderson G.; Footer M.; Hultgren S. *PNAS* **2004**, *101*, 1333-8]. All radioactivity measurements have been corrected for decay.

3 µg	%IA/G					60 µg %IA/G	300 µg %IA/G
Time	30 min	1h	3h	6h	24h	30 min	30 min
Heart	4.08± 0.85	3.66± 0.96	2.93± 0.26	2.91± 0.29	3.27± 0.26	1.80± 0.34	0.96± 0.16
Lungs	2.33± 0.42	2.34± 0.44	1.69± 0.23	1.93± 0.36	1.58± 0.09	1.64± 0.32	1.49± 0.29
Liver	6.50± 1.26	5.56± 0.77	4.98± 0.45	5.10± 0.63	5.69± 0.50	4.26± 0.36	2.43± 0.14
KidneyL	3.83± 0.80	1.89± 0.26	1.57± 0.08	1.64± 0.20	1.51± 0.28	3.07± 1.04	4.36± 0.38
KidneyR	3.33± 0.41	1.98± 0.41	1.61± 0.15	1.46± 0.12	1.44± 0.26	4.72± 2.80	4.00± 0.70
Blood	0.66± 0.19	0.27± 0.02	0.21± 0.01	0.18± 0.04	0.10± 0.01	0.77± 0.09	1.45± 0.34
Bladder	5.06± 4.21	2.92± 1.36	1.37± 0.17	1.39± 0.24	2.08± 0.79	1.22± 0.46	2.19± 2.82

Table S2. Activities of **5** in mouse organs.

Liver and heart demonstrate an almost stable activity of **5** over 24h. Increasing the dose of **5** decreases their percentage of activity (30 min. time point), whereas the percentage increases in the blood. This means that **5** is retained less in the liver and heart but more in the blood before being filtered through the kidneys into the bladder. Higher doses of **5** thus give rise to higher concentrations of the β -CD derivatives in the bladder.

Procedure for *in vivo* experiments

A murine model of urinary tract infection was used to test the ability of the compounds to inhibit the colonization of UTI89 in the bladder [Hung C.S.; Dodson, K.W., Hultgren S.J. *Nat. Protoc.* **2009**, 4, 1230-1243 and Wellens A.; Garofalo C.; Nguyen H.; Van Gerven N.; Slättegård R.; Hernalsteens, J.-P.; Wyns, L.; Oscarson, S.; De Greve H.; Hultgren S.J.; Bouckaert, J. *PLoS ONE* **2008**, 3, e2040]. The solution with high concentration of compounds was added to the resuspension of UTI89 before given to the mice. The eight-week old Female C3H/HeN mice (Harlan, Horst, The Netherlands) were anesthetized and infected via transurethral catheterization of 10^7 CFU UTI89 in solution in PBS, or in PBS with the compound in the mentioned concentration. The mice were sacrificed at 24 hours post infection and the bladders were harvested, homogenized and resuspended in PBS. The serial dilutions were spot on LB medium agar plates. The bacterial load was determined by counting the CFU recovered from the bladder. The animal experiments were approved by the Ethical Committee for Animal Experiments of Vrije Universiteit Brussel and complied with all relevant national legislation and institutional policies. The Mann-Whitney test was applied for the comparison of the data obtained from the untreated group and inhibition group in GraphPad Prism version 5.1 and two tailed P value were shown (GraphPad software).